

Interaction Notes

Note 179

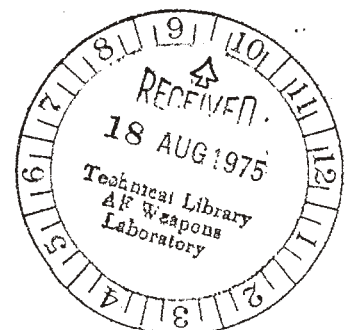
May 1974

Quasi-Static Magnetic Field Penetration into a
Hemispherical Indentation in an Infinite
Conducting Plane

John Lam
The Dikewood Corporation
Albuquerque, New Mexico

Abstract

The problem of the penetration of a quasi-static magnetic field into a hemispherical indentation in an infinite conducting plane is formulated as an integral equation, and solved numerically to a high degree of accuracy. The results are directly applicable to the study of a large class of aircraft antennas, such as the marker beacon antenna. The value of the magnetic potential inside the cavity, the induced magnetic dipole moment, and the magnetic flux passing through a receiving loop antenna erected in the cavity are calculated.



I. Introduction

Many aircraft receiving antennas are housed in cavities indented directly on the metallic aircraft skin. To analyse the performance of such antennas, it is important to understand the manner in which an incoming electromagnetic signal enters the cavities. Very often the antennas are electrically small; and a quasi-static analysis is applicable. We have recently solved exactly the problem of quasi-static electric field penetration into a hemispherical cavity in an infinite conducting plane [1]. Having closed the electrostatic problem, we turn to its magnetostatic counterpart.

The exact solution of the electrostatic problem was effected by a skillful inversion transformation which, unfortunately, is of little use to the magnetostatic case because of the difference in boundary conditions. Accordingly, we seek a different approach and formulate the present problem as an integral equation. A highly accurate - and in fact practically exact - solution is constructed from physical considerations. The solution is used to compute the magnetic potential, the induced magnetic dipole moment, and the magnetic flux through a loop antenna in the cavity. These results, together with those in the companion report [1], are directly applicable to the analysis of the excitation of electrically small stub and loop antennas in metallic cavities by external electromagnetic signals.

The two-dimensional problem of quasi-static field penetration into a rectangular trough has been solved in a report by Marin [2].

II. Statement of the Problem

We consider a perfect conductor occupying the half-space $z > 0$, except for a hemispherical indentation of radius a centered at the coordinate origin (see Fig. 1). It is excited by a uniform external magnetic field \underline{H}_0 which, in the quasi-static limit, must of necessity be tangential to the conductor surface at large distances from the cavity; and we can set

$$\underline{H}_0 = H_0 \hat{x}. \quad (1)$$

It can be derived from the magnetic source potential

$$U_0 = -H_0 x \quad (2)$$

through the relation

$$\underline{H}_0 = -\nabla U_0. \quad (3)$$

As is well-known, the magnetostatic problem consists of finding the total magnetic potential U such that it is a solution of the Laplace equation in free space, its normal derivative vanishes on the conductor, it reduces to U_0 at large distances from the cavity, and that it has no singularities in finite space. The last condition guarantees the absence of true sources except at infinity.

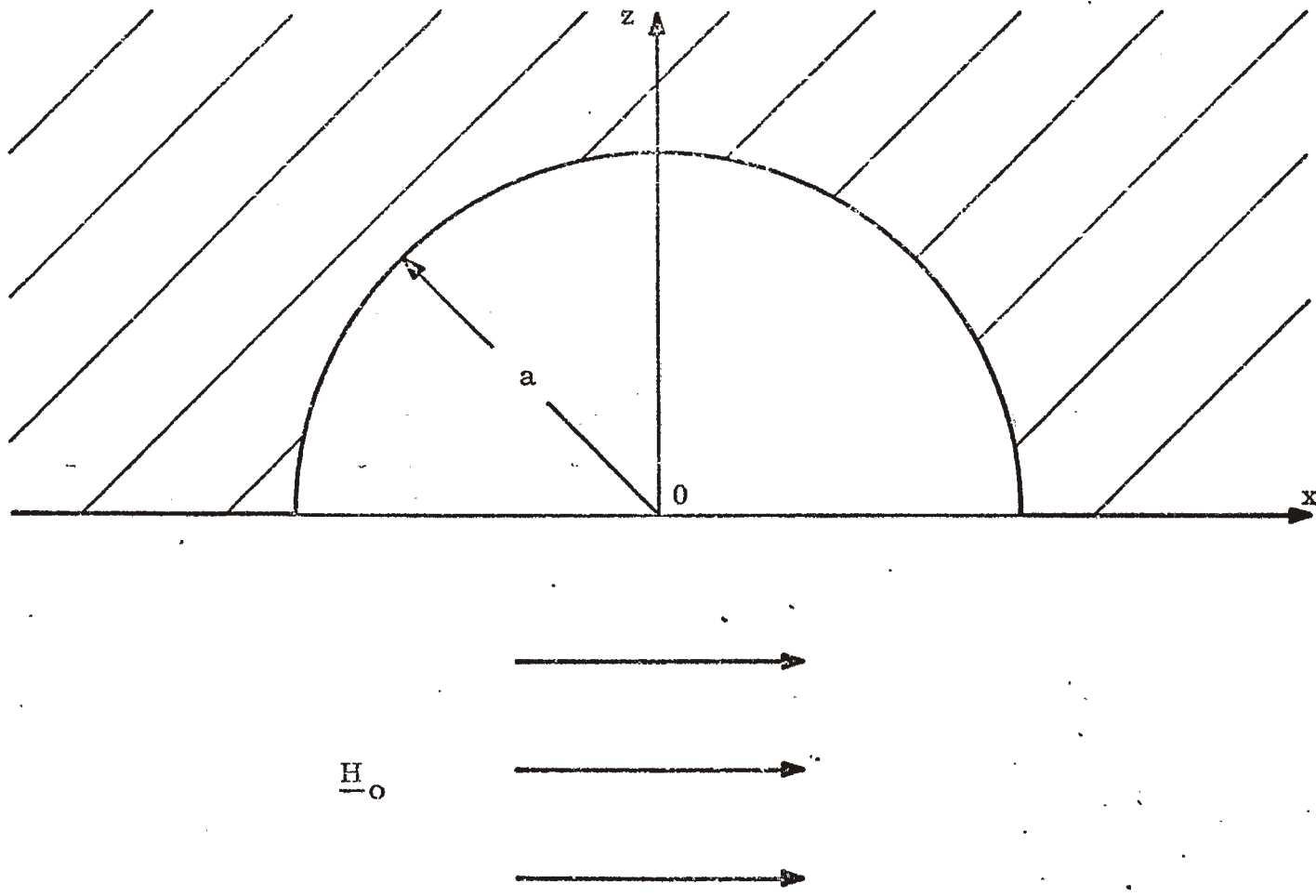


Fig. 1.-- Geometry of the problem.

III. Derivation of the Integral Equation

To facilitate the construction of mathematical expressions for the set of conditions just enunciated, we introduce an imaginary hemispherical surface S defined by

$$r = a, \quad \pi/2 < \theta < \pi, \quad (4)$$

where r and θ , together with ϕ , are the standard spherical polar coordinates. S is clearly the spherical complement of the hemispherical cavity wall (see Fig. 2). It divides free space into two regions: the sphere with radius a will be called region 1; its exterior, excluding the conductor, will be called region 2. In terms of r, θ and ϕ , U_0 in (2) becomes

$$U_0(r, \theta, \phi) = -H_0 r \sin \theta \cos \phi. \quad (5)$$

By symmetry the total potential U must have the same ϕ -dependence as U_0 . We expand U in terms of suitable harmonic functions in regions 1 and 2 separately, distinguishing the two cases by the suffixes 1 and 2 respectively:

$$U_1(r, \theta, \phi) = H_0 a \sum_{n=1}^{\infty} A_n \left(\frac{r}{a}\right)^n P_n^1(\cos \theta) \cos \phi, \quad (6)$$

$$U_2(r, \theta, \phi) = U_0 + H_0 a \sum_{\substack{m=1 \\ \text{odd}}}^{\infty} B_m \left(\frac{a}{r}\right)^{m+1} P_m^1(\cos \theta) \cos \phi, \quad (7)$$

where P_n^1 is an associated Legendre function. U_1 and U_2 are just different incarnations of the total potential U . By construction they are

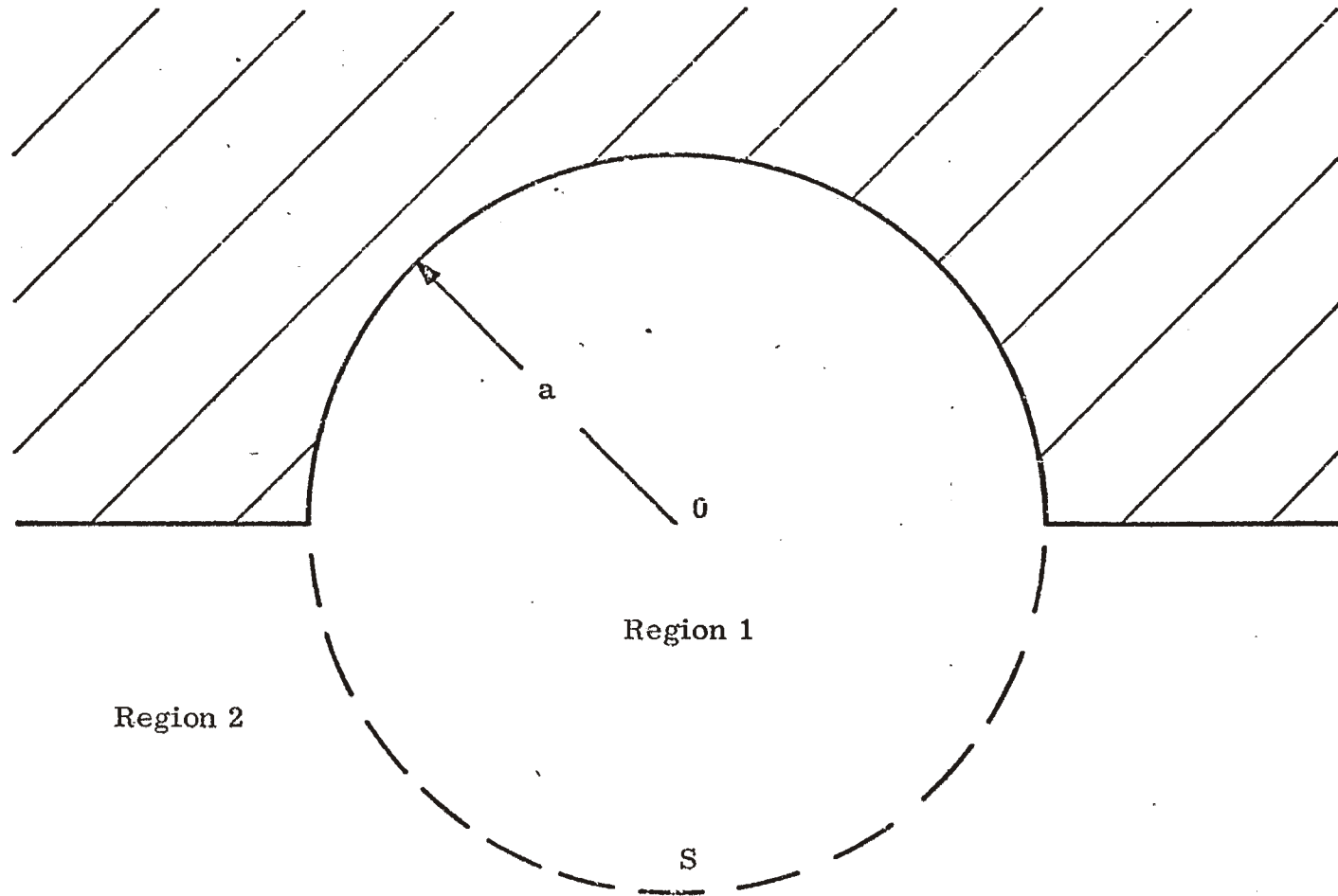


Fig. 2.-- Division of free space into regions 1 and 2 by the imaginary hemispherical surface S.

both regular solutions of the Laplace equation; and U_2 tends to U_0 at infinity. The summation over m is limited to odd integers to make the normal derivation of U_2 vanish on the entire flange of the cavity. With so many conditions already built into (6) and (7), the coefficients A_n and B_m are determined entirely by conditions on the spherical surface $r = a$.

Let the radial derivative of U on S be

$$\frac{\partial U}{\partial r} = H_0 f(\theta) \cos \phi, \quad r = a, \quad \pi/2 < \theta < \pi, \quad (8)$$

where $f(\theta)$ is as yet unknown. We must necessarily have

$$f(\pi) = 0, \quad (9)$$

or else the expression (8) has a ϕ -dependence even at $\theta = \pi$, which is absurd. Since S is only an imaginary surface, the potential and its normal derivative must be continuous across it. We are led to the following three boundary conditions at $r = a$:

$$\begin{aligned} \text{(i)} \quad \frac{\partial U_1}{\partial r} &= 0, & 0 < \theta < \pi/2, \\ &= H_0 f(\theta) \cos \phi, & \pi/2 < \theta < \pi, \end{aligned} \quad (10)$$

$$\text{(ii)} \quad \frac{\partial U_2}{\partial r} = H_0 f(\theta) \cos \phi, \quad \pi/2 < \theta < \pi, \quad (11)$$

$$\text{(iii)} \quad U_1 = U_2 \quad \pi/2 < \theta < \pi. \quad (12)$$

Substituting (6) into (10) and using the orthogonality relation of the associated Legendre functions in the interval $0 < \theta < \pi$:

$$\int_0^{\pi} d\theta \sin \theta P_n^1(\cos \theta) P_{n'}^1(\cos \theta) = \frac{2n(n+1)}{2n+1} \delta_{nn'} \quad (13)$$

we obtain

$$A_n = \frac{2n+1}{2n^2(n+1)} \int_{\pi/2}^{\pi} d\theta \sin \theta f(\theta) P_n^1(\cos \theta). \quad (14)$$

Similarly, substituting (7) into (11) and using the orthogonality relation in the interval $\pi/2 < \theta < \pi$:

$$\int_{\pi/2}^{\pi} d\theta \sin \theta P_m^1(\cos \theta) P_{m'}^1(\cos \theta) = \frac{m(m+1)}{2m+1} \delta_{mm'}, \quad m, m' \text{ odd} \quad (15)$$

we obtain

$$B_m = \frac{1}{2} \delta_{m1} - \frac{2m+1}{m(m+1)^2} \int_{\pi/2}^{\pi} d\theta \sin \theta f(\theta) P_m^1(\cos \theta). \quad (16)$$

From (14) and (16) it is clear that finding the function $f(\theta)$ in (8) is equivalent to solving our present magnetostatic potential problem. Let us derive an integral equation for it. Even if we insert an arbitrary $f(\theta)$ in (14) and (16), the potentials U_1 and U_2 in (6) and (7) so constructed will still satisfy the boundary condition on the conductor, the asymptotic condition at infinity, as well as the continuity condition of the radial derivatives on S . The true and unique $f(\theta)$, however, is determined by the remaining third boundary condition (12). Substituting (14) and (16)

in (6) and (7), and the latter two in turn in (12), and interchanging the orders of summation and integration, we obtain the following first-kind integral equation for $f(\theta)$:

$$\int_{\pi/2}^{\pi} d\theta' \sin\theta' K(\theta, \theta') f(\theta') = -\frac{3}{2} \sin\theta, \quad \pi/2 < \theta < \pi, \quad (17)$$

where

$$K(\theta, \theta') = K_1(\theta, \theta') + K_2(\theta, \theta'), \quad (18)$$

$$K_1(\theta, \theta') = \sum_{n=1}^{\infty} \frac{2n+1}{2n^2(n+1)} P_n^1(\cos\theta) P_n^1(\cos\theta'), \quad (19)$$

$$K_2(\theta, \theta') = \sum_{\substack{m=1 \\ \text{odd}}}^{\infty} \frac{2m+1}{m(m+1)^2} P_m^1(\cos\theta) P_m^1(\cos\theta'). \quad (20)$$

IV. Evaluation of the Kernel

We can expect the kernel $K(\theta, \theta')$ to exhibit one type of divergence or another. As a first step towards solving the integral equation (17), we evaluate K in closed form and analyse its singularities. From the addition theorem

$$P_n(\cos \alpha) = P_n(\cos \theta) P_n(\cos \theta') + 2 \sum_{m=1}^n \frac{(n-m)!}{(n+m)!} P_n^m(\cos \theta) P_n^m(\cos \theta') \cos m \phi \quad (21)$$

where

$$\cos \alpha = \cos \theta \cos \theta' + \sin \theta \sin \theta' \cos \phi, \quad (22)$$

we obtain, after multiplying both sides of (21) by $\cos \phi$ and integrating over ϕ from 0 to π , the relation

$$P_n^1(\cos \theta) P_n^1(\cos \theta') = \frac{n(n+1)}{\pi} \int_0^\pi d\phi \cos \phi P_n(\cos \alpha). \quad (23)$$

Then (19) and (20) become

$$K_1(\theta, \theta') = \frac{1}{2\pi} \int_0^\pi d\phi \cos \phi \sum_{n=1}^{\infty} \left(2 + \frac{1}{n}\right) P_n(\cos \alpha), \quad (24)$$

$$K_2(\theta, \theta') = \frac{1}{\pi} \int_0^\pi d\phi \cos \phi \sum_{\substack{m=1 \\ \text{odd}}}^{\infty} \left(2 - \frac{1}{m+1}\right) P_m(\cos \alpha). \quad (25)$$

Let us consider the infinite sum in (24). From the generating function of the Legendre polynomials

$$\frac{1}{\sqrt{1 - 2h \cos \alpha + h^2}} = \sum_{n=0}^{\infty} h^n P_n(\cos \alpha), \quad (26)$$

we have for $h = 1$

$$\sum_{n=1}^{\infty} P_n(\cos \alpha) = \frac{1}{\sqrt{2(1-\cos \alpha)}} - 1. \quad (27)$$

Dividing (26) throughout by h and integrating over h from 0 to 1, we get

$$\sum_{n=1}^{\infty} \frac{1}{n} P_n(\cos \alpha) = \ln \left(\frac{2}{1 - \cos \alpha + \sqrt{2(1-\cos \alpha)}} \right). \quad (28)$$

Substituting (27) and (28) into (24) we obtain

$$K_1(\theta, \theta') = \frac{1}{2\pi} \int_0^{\pi} d\phi \cos \phi \left(\frac{2}{\sqrt{2(1-\cos \alpha)}} - \ln \left[1 - \cos \alpha + \sqrt{2(1-\cos \alpha)} \right] \right). \quad (29)$$

The sum in (25) can be evaluated in a similar fashion. The odd-integer sum can be extracted from (26) by changing the sign of h . The result is

$$K_2(\theta, \theta') = \frac{1}{2\pi} \int_0^{\pi} d\phi \cos \phi \left(\frac{2}{\sqrt{2(1-\cos \alpha)}} - \frac{2}{\sqrt{2(1+\cos \alpha)}} - \ln \left(\frac{1 - \cos \alpha + \sqrt{2(1-\cos \alpha)}}{1 - \cos \alpha} \right) - \ln \left(\frac{-1 - \cos \alpha + \sqrt{2(1+\cos \alpha)}}{1 - \cos \alpha} \right) \right). \quad (30)$$

It is easy to see that both $K_1(\theta, \theta')$ and $K_2(\theta, \theta')$ have logarithmic divergences at $\theta = \theta'$, because the leading terms of the integrands in (29) and (30) diverge linearly at one limit of integration or the other when $\theta = \theta'$. As we are going to solve the integral equation numerically in the next section, it is imperative that we pacify these divergences in some efficient manner in advance. Take for example the integral

$$\int_0^{\pi} d\phi \frac{\cos \phi}{\sqrt{1 - \cos \alpha}} = \int_0^{\pi} d\phi \frac{\cos \phi}{\sqrt{A - B \cos \phi}}, \quad (31)$$

where, by (22),

$$\begin{aligned} A &= 1 - \cos \theta \cos \theta' \geq 0, \\ B &= \sin \theta \sin \theta' \geq 0, \quad \pi/2 < \theta, \theta' < \pi. \end{aligned} \quad (32)$$

Let us split up the integral as follows:

$$\int_0^{\pi} d\phi \frac{\cos \phi}{\sqrt{A - B \cos \phi}} = \int_0^{\pi} \frac{d\phi}{\sqrt{A - B \cos \phi}} - \int_0^{\pi} d\phi \frac{1 - \cos \phi}{\sqrt{A - B \cos \phi}}. \quad (33)$$

The second integral on the right-hand side is regular. The logarithmic divergence at $\theta = \theta'$ is isolated in the first integral which can be expressed in terms of the complete elliptic integral of the first kind:

$$\int_0^{\pi} \frac{d\phi}{\sqrt{A - B \cos \phi}} = \frac{2}{\sqrt{A+B}} K\left(\sqrt{\frac{2B}{A+B}}\right), \quad (34)$$

where

$$K(k) = \int_0^{\pi/2} \frac{d\phi}{\sqrt{1-k^2 \sin^2 \phi}}, \quad 0 \leq k < 1. \quad (35)$$

(The complete elliptic integral $K(k)$ is not to be confused with the kernel $K(\theta, \theta')$!) It is well-known that $K(k)$ diverges logarithmically as $k \rightarrow 1$. Therefore the integral (34) diverges for $A=B$ or, by (32), for $\theta = \theta'$.

A similar manipulation can be applied to the integral

$$\int_0^{\pi} d\phi \frac{\cos \phi}{\sqrt{1 + \cos \alpha}} \quad (36)$$

in (30). Gathering all the results, we can express the total kernel

$K = K_1 + K_2$ in the form

$$K(\theta, \theta') = \Lambda_1(\theta, \theta') + \Lambda_2(\theta, \theta') + L(\theta, \theta'), \quad (37)$$

$$\Lambda_1(\theta, \theta') = \frac{1}{\pi} \frac{2\sqrt{2}}{\sqrt{1 - \cos(\theta + \theta')}} K\left(\sqrt{\frac{2 \sin \theta \sin \theta'}{1 - \cos(\theta + \theta')}}\right), \quad (38)$$

$$\Lambda_2(\theta, \theta') = \frac{1}{\pi} \frac{\sqrt{2}}{\sqrt{1 + \cos(\theta - \theta')}} K\left(\sqrt{\frac{2 \sin \theta \sin \theta'}{1 + \cos(\theta - \theta')}}\right), \quad (39)$$

$$L(\theta, \theta') = -\frac{1}{\pi} \int_0^{\pi} d\phi \left[\frac{2(1 - \cos \phi)}{\sqrt{2(1 - \cos \alpha)}} + \frac{1 + \cos \phi}{\sqrt{2(1 + \cos \alpha)}} + \right. \\ \left. + \cos \phi \ln \left\{ \left(\frac{2}{\sqrt{2(1 - \cos \alpha)}} + 1 \right) \left(\sqrt{2(1 + \cos \alpha)} - 1 - \cos \alpha \right)^{1/2} \right\} \right], \quad (40)$$

where $\cos \alpha$ is defined in (22).

The tortuous passage from (29) and (30) to (37), (38), (39), and (40) should not be dismissed outright as a mere exercise in algebraic futility,

despite the more complex appearance of the latter expressions, since we can now make good use of the polynomial approximation for the complete elliptic integral:

$$K(k) \approx (a_0 + a_1 \lambda + a_2 \lambda^2) - (b_0 + b_1 \lambda + b_2 \lambda^2) \ln \lambda, \quad (41)$$

where

$$\lambda = 1 - k^2,$$

$$\begin{aligned} a_0 &= 1.3862944, & b_0 &= 0.5 \\ a_1 &= 0.1119723, & b_1 &= 0.1213478, \\ a_2 &= 0.0725296, & b_2 &= 0.0288729. \end{aligned} \quad (42)$$

The error is less than $0.00003^{[3]}$. The surviving integral $L(\theta, \theta')$ in (40) can be easily evaluated on the computer, since its integrand has at most logarithmic singularities at the limits of integration.

V. Numerical Solution of the Integral Equation

There are more than one way to solve the integral equation (17) numerically, and we will choose the best one. We will construct a trial solution from physical considerations, and the parameters of the trial solution are determined to satisfy the integral equation. This method is the best since the solution $f(\theta)$ is expected on physical ground to diverge at the rim of the cavity, and we can represent this divergence faithfully with a well-chosen form of the trial solution.

It is clear from (8) that the function $f(\theta)$ is proportional to the radial component of the total magnetic field on the imaginary hemispherical surface S . Let us digress a little, and for a few moments delve into the nature of the divergence of magnetic fields at sharp conducting edges. Let us consider the immediate neighborhood of the edge of a conducting wedge of exterior angle β , and let us set up a local cylindrical polar coordinate system $(\bar{\rho}, \bar{\phi}, \bar{z})$ such that the \bar{z} -axis is tangential to the edge and that the two wedge surfaces are given by $\bar{\phi} = 0$ and β . If we are close enough to the edge, variations in \bar{z} can be ignored. The magnetic potential satisfies a two-dimensional Laplace equation in $\bar{\rho}$ and $\bar{\phi}$. The condition of perfect conductivity requires the vanishing of the normal derivative on both wedge surfaces. Then the potential can be expanded in the form

$$a_0 + a_1 \bar{\rho}^t \cos(t\bar{\phi}) + a_2 \bar{\rho}^{2t} \cos(2t\bar{\phi}) + \dots, \quad (43)$$

where

$$t = \frac{\pi}{\beta}. \quad (44)$$

As a consequence both the $\bar{\rho}$ - and $\bar{\phi}$ -components of the magnetic field behave near the edge like $\bar{\rho}^{-1}$. For $\beta < \pi$, they are finite; but for a sharp edge with $\beta > \pi$, they diverge. In our hemispherical cavity problem, $\beta = 3\pi/2$, hence we can expect a divergence like $\bar{\rho}^{-1/3}$.

The above considerations suggest a trial solution for (17) in the form

$$f(\theta) = -\sin\theta \left(\frac{c_1}{|\cos\theta|^{1/3}} + c_2 |\cos\theta|^{1/3} \right), \quad (45)$$

since $\bar{\rho}$ in (43) becomes a $|\cos\theta|$ in our case. c_1 and c_2 are adjustable constants. The term in c_2 represents the effect of the third and subsequent terms in (43). The factor $-\sin\theta$ serves the dual purpose of providing an overall envelope which imitates the incident part in (5), and of insuring the satisfaction of condition (9).

We substitute (45) into the left-hand side of (17) and evaluate the integral numerically on the computer for the two values $\cos\theta = -0.2$ and -0.8 . To avoid having the logarithmic singularity of the kernel $K(\theta, \theta')$ inside the range of integration we break up the integral into two parts; thus

$$\int_{\pi/2}^{\pi} d\theta' \sin\theta' K(\theta, \theta') f(\theta') = \int_{\pi/2}^{\theta} + \int_{\theta}^{\pi} \quad (46)$$

The constants c_1 and c_2 are adjusted to satisfy the integral equation (17) at these two chosen values of $\cos\theta$. The result is

$$f(\theta) = -\sin \theta \left(\frac{0.55100}{|\cos \theta|^{1/3}} + 0.51154 |\cos \theta|^{1/3} \right). \quad (47)$$

When this $f(\theta)$ is resubstituted into (17), we find that it practically satisfies the integral equation uniformly. The discrepancy between the two sides is well within 1% throughout the entire interval $\pi/2 < \theta < \pi$. In real life we seldom fuss over an error of this order. The solution is quasi-exact, and we really hit the nail on the head with our intuitively constructed trial solution (45). The explicit solution (47) is plotted in Fig. 3 and compared with its incident part $-\sin \theta$.

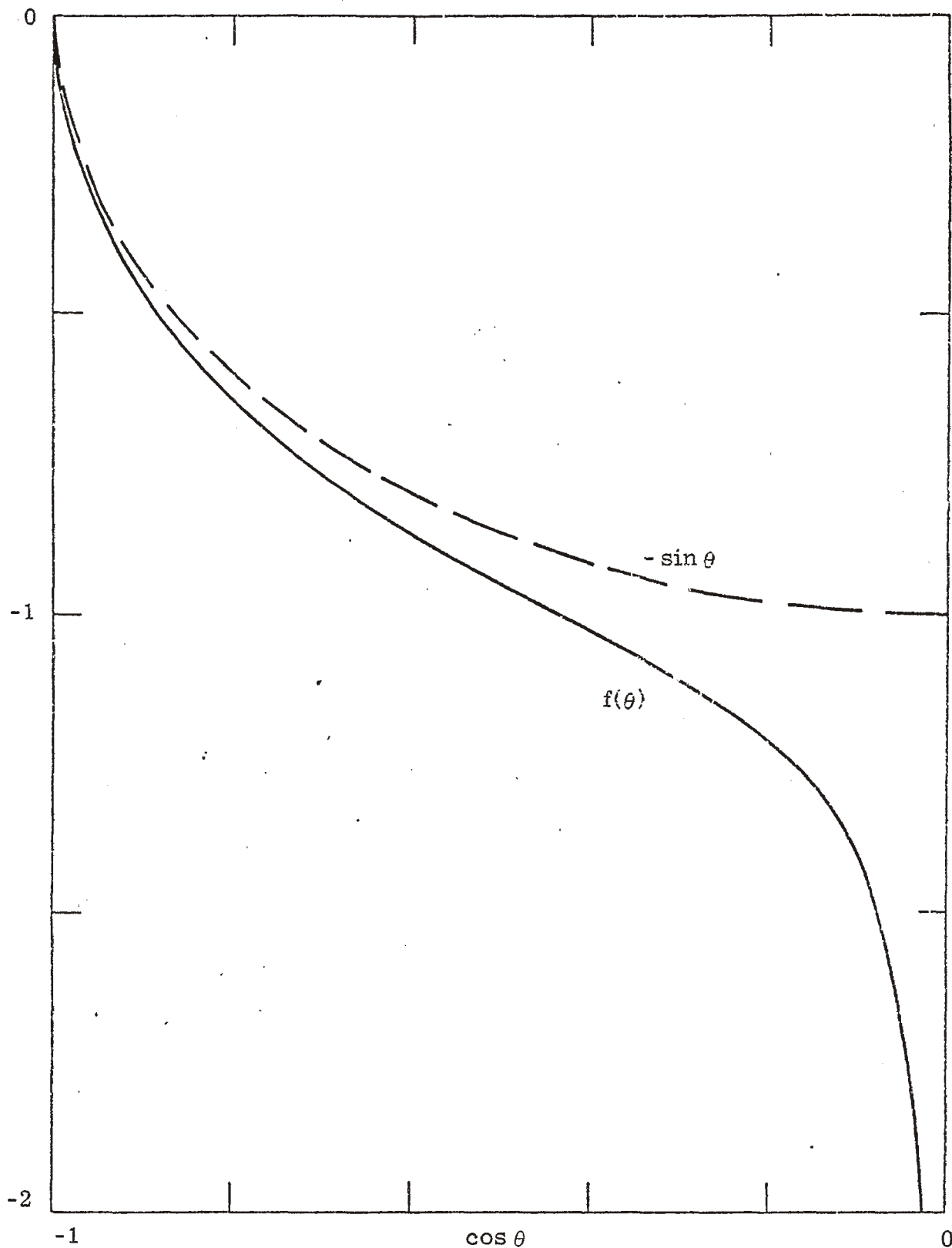


Fig. 3. -- Solution $f(\theta)$ of the integral equation (17) as compared with its incident part $-\sin \theta$ (broken line).

VI. Potential in the Cavity

We proceed to calculate the value of the total magnetic potential in the cavity. For this purpose we need only the potential U_1 in region 1 given by (6). Putting (14) into (6) we obtain

$$U_1(r, \theta, \phi) = H_0 a \cos \phi \int_{\pi/2}^{\pi} d\theta' \sin \theta' f(\theta') \sum_{n=1}^{\infty} \frac{2n+1}{2n^2(n+1)} \left(\frac{r}{a}\right)^n P_n^1(\cos \theta) P_n^1(\cos \theta'), \quad (48)$$

The infinite sum can be evaluated in closed form by the method in Section IV. Here we set h in (26) and its derived expressions equal to r/a instead of 1. The result reads

$$U_1(r, \theta, \phi) = H_0 a u(r, \theta) \cos \phi, \quad (49)$$

$$u(r, \theta) = \int_{\pi/2}^{\pi} d\theta' \sin \theta' f(\theta') W(r, \theta, \theta'), \quad (50)$$

$$W(r, \theta, \theta') = \frac{1}{2\pi} \int_0^{\pi} d\phi \cos \phi \left[\frac{2}{\sqrt{1 - 2 \frac{r}{a} \cos \alpha + \left(\frac{r}{a}\right)^2}} - \ln \left(1 - \frac{r}{a} \cos \alpha + \sqrt{1 - 2 \frac{r}{a} \cos \alpha + \left(\frac{r}{a}\right)^2} \right) \right], \quad (51)$$

where $\cos \alpha$ is defined as in (22). Using the solution (47) we evaluate U_1 numerically for $\phi=0$, and the results are tabulated in Table 1. We have used a uniform net of field points most conveniently specified by the cylindrical polar coordinates

$$\rho = r \sin \theta, \quad z = r \cos \theta. \quad (52)$$

For other values of ϕ , the tabulated values must be multiplied throughout by $\cos \phi$.

The computed results for $\phi = 0$ are also plotted in Fig. 4. The intersections of the equipotential surfaces with the x-z plane, that is, for $\phi = 0$ and π , are sketched in Fig. 5.

Table 1. Total magnetic potential U_1 in the cavity in units of $H_0 a$ for $\phi = 0$ ($\rho = r \sin \theta$, $z = r \cos \theta$). For other values of ϕ , the entries should be multiplied by $\cos \phi$.

ρ/a z/a	0.0	0.1	0.2	0.3	0.4	0.5	0.6	0.7	0.8	0.9
0.9	0.000	-0.025	-0.049	-0.073	-0.095					
0.8	0.000	-0.027	-0.054	-0.081	-0.106	-0.130	-0.153			
0.7	0.000	-0.030	-0.061	-0.090	-0.118	-0.145	-0.171	-0.193		
0.6	0.000	-0.034	-0.068	-0.101	-0.133	-0.163	-0.191	-0.217	-0.239	
0.5	0.000	-0.038	-0.076	-0.113	-0.149	-0.183	-0.215	-0.244	-0.269	
0.4	0.000	-0.043	-0.085	-0.127	-0.167	-0.206	-0.243	-0.276	-0.305	-0.329
0.3	0.000	-0.048	-0.095	-0.142	-0.188	-0.232	-0.275	-0.314	-0.349	-0.376
0.2	0.000	-0.053	-0.105	-0.158	-0.210	-0.261	-0.311	-0.358	-0.401	-0.436
0.1	0.000	-0.058	-0.116	-0.175	-0.233	-0.291	-0.349	-0.406	-0.462	-0.512
0.0	0.000	-0.064	-0.127	-0.191	-0.256	-0.321	-0.388	-0.456	-0.528	-0.606

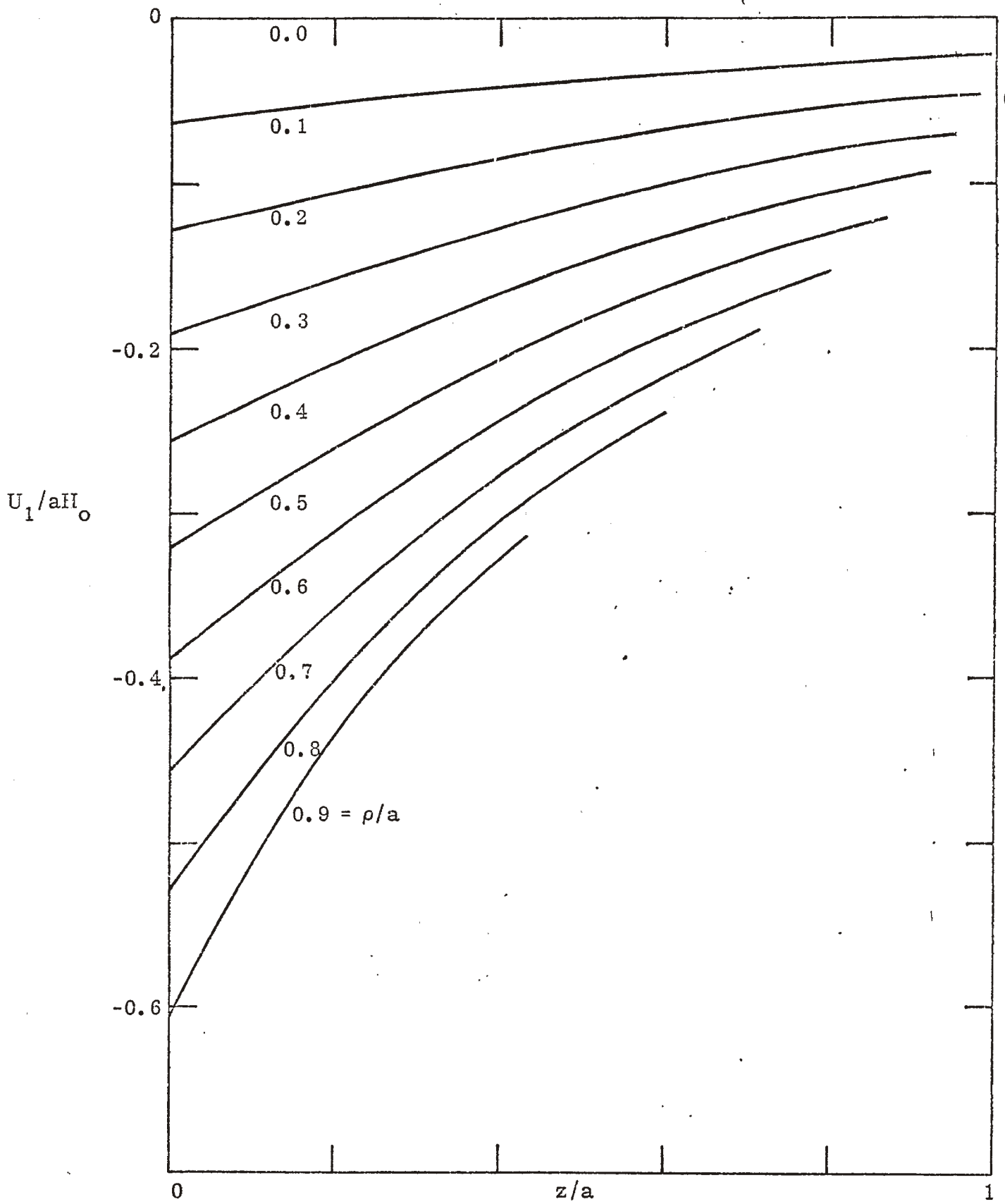


Fig. 4.-- Total magnetic potential U_1 in the cavity in units of aH_0 for $\phi = 0$ ($\rho = r \sin \theta$, $z = r \cos \theta$). The curves terminate on the right at the cavity wall.

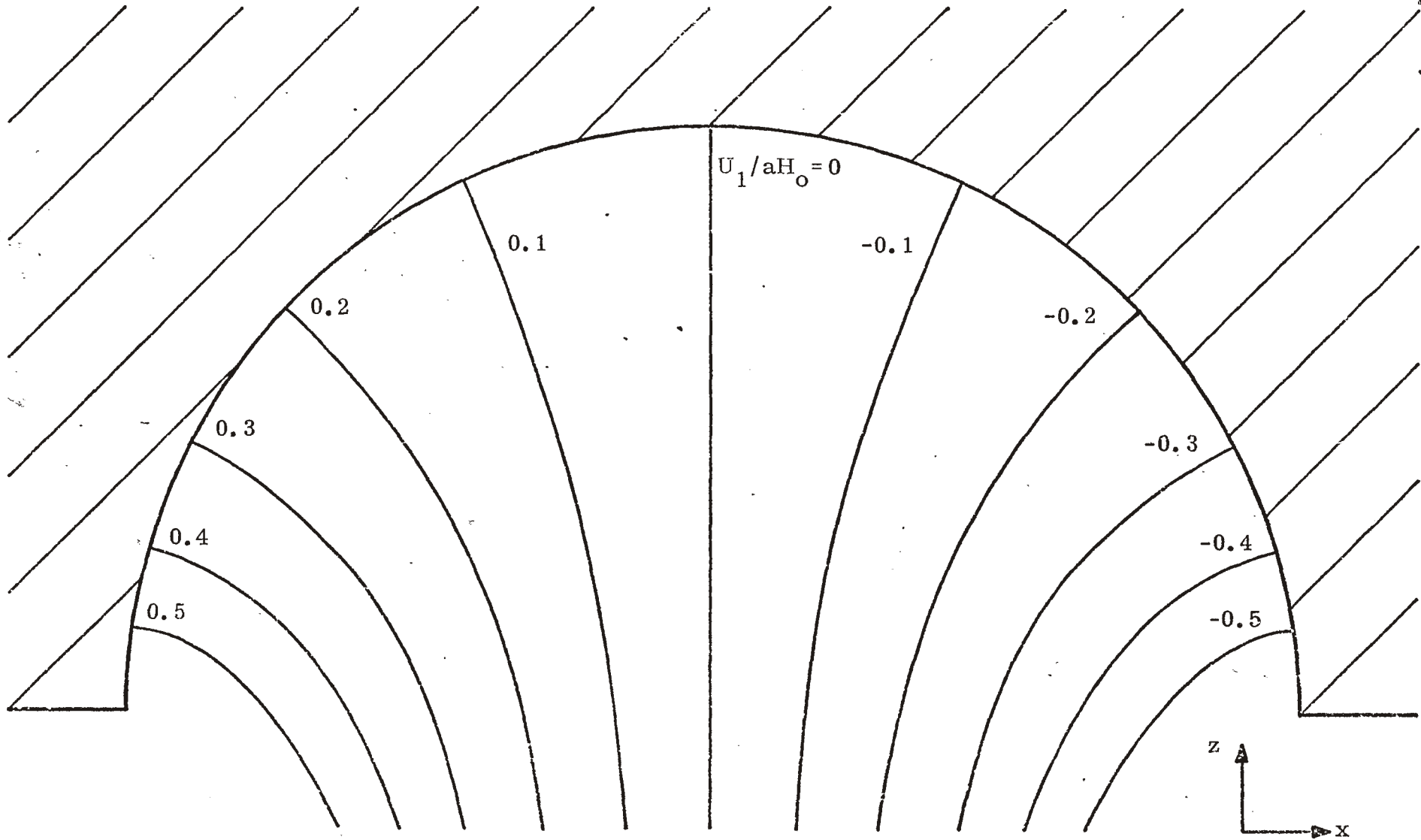


Fig. 5. -- Intersections of the equipotential surfaces with the x - z plane (i. e., $\phi = 0$ and π). For other values of ϕ the surfaces are more fanned out due to the factor $\cos \phi$.

VII. Induced Magnetic Dipole Moment

Let us consider the behavior of the total potential at large distances from the cavity. From (7) we have

$$U_2 \approx U_0 - H_0 a^3 B_1 \frac{\sin \theta \cos \phi}{r^2}, \quad r \gg a. \quad (53)$$

The last term characterizes the far zone behavior of the induced potential, and is of a dipole form. We can define an induced magnetic dipole moment \underline{m} such that

$$U_2 \approx U_0 + \frac{1}{4\pi} \frac{\underline{m} \cdot \underline{r}}{r^3}. \quad (54)$$

Comparing (53) and (54) we obtain

$$\underline{m} = \alpha_m \underline{H}_0, \quad \alpha_m = -4\pi B_1 a^3. \quad (55)$$

From (16) we have

$$B_1 = \frac{1}{2} + \frac{3}{4} \int_{\pi/2}^{\pi} d\theta \sin^2 \theta f(\theta). \quad (56)$$

For $f(\theta)$ given by (47) the integration is trivial, and we obtain

$$\alpha_m \approx 1.73 a^3. \quad (57)$$

This is to be compared with the finding in the more readily soluble problem of a hemispherical boss, where $\alpha_m = -2\pi a^3$. Comparing again the present result with that from our companion electrostatic calculations [1], we note that the electric and magnetic polarizabilities of the hemispherical cavity

differ in sign. The same observation holds also for the case of the hemispherical boss.

With an induced magnetic dipole moment determined from (57), the total magnetic potential U_2 differs from the incident potential U_0 by less than 1% for $r \gtrsim 2.4a$.

VIII. Magnetic Flux

Suppose a thin conducting wire is stretched from one side of the cavity wall to the other. Then, together with the conducting cavity wall, it constitutes a loop antenna which can be excited by temporal variations in the magnetic field fluxing through it. It is desirable to calculate the magnetic flux passing between the wire and the cavity wall.

Let the wire be perpendicular to the z-axis, lying in a plane which contains the z-axis and which makes an angle ϕ with the x-z plane. It is depicted as the straight line MN in Fig. 6. Let D be its distance from the zenith of the cavity (or nadir, depending on one's preferred point of view). We wish to calculate the magnetic flux through the dotted area in Fig. 6.

It is clear that the flux is due entirely to the ϕ -component of the magnetic field. From (49) we have

$$H_{\phi} = - \frac{1}{r \sin \theta} \frac{\partial U_1}{\partial \phi} = H_0 a \sin \phi \frac{u(r, \theta)}{r \sin \theta} . \quad (58)$$

By symmetry the total flux is twice that through, say, the right half of the dotted area in Fig. 6, for which we can take $0 < \phi < \pi$. Moreover, it is sufficient to consider the case $\phi = \pi/2$ when the antenna loop is normal to the incident magnetic field \underline{H}_0 . For other orientations the flux is diminished by a factor $\sin \phi$. For $\phi = \pi/2$ the total flux Φ through the entire dotted area is given by

$$\Phi = 2\mu_0 \iint dA H_x = -2\mu_0 \iint dA H_{\phi} \Big|_{\phi = \pi/2} , \quad (59)$$

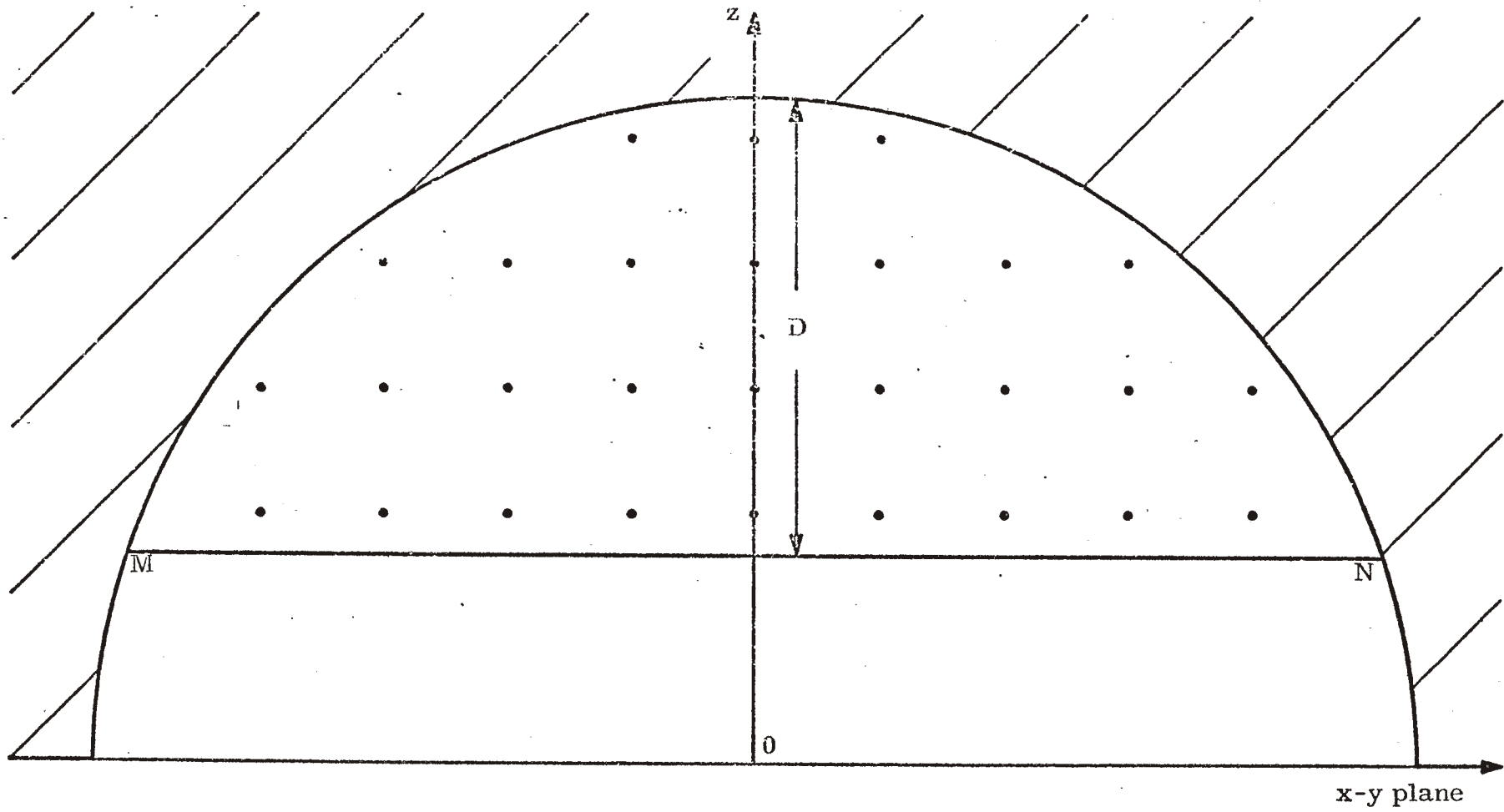


Fig. 6. -- Geometry of the magnetic flux calculation.

where the surface integral goes over the right half of the dotted area in Fig. 6. Substituting (58) into (59) we have

$$\Phi = -2\mu_0 H_0 a \int_{a-D}^a dz \int_0^{\sqrt{a^2-z^2}} \frac{d\rho}{\rho} u(r,\theta), \quad (60)$$

where the connection between (ρ, z) and (r, θ) are as in (52). The expression (60) is evaluated numerically on the computer, with $u(r, \theta)$ obtained from Table 1 by interpolation. The results are plotted against D in Fig. 7.

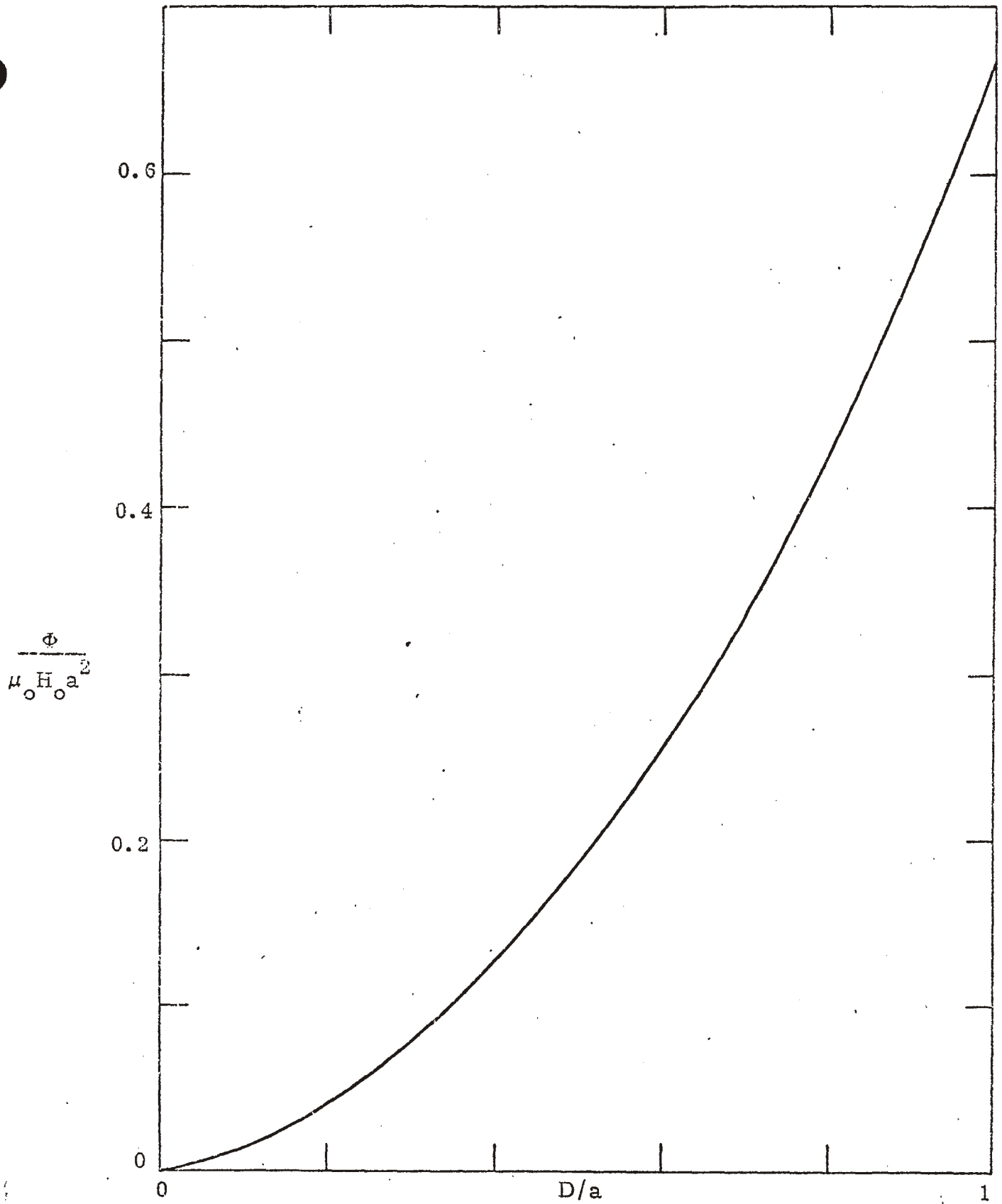


Fig. 7. -- Total magnetic flux Φ versus the distance D of a wire from the cavity bottom for $\phi = \pi/2$. For other values of ϕ ($0 < \phi < \pi$), Φ is diminished by a factor $\sin \phi$.

Acknowledgment

Thanks are due to Dr. K. S. H. Lee for many discussions on the problem.

References

- [1] J. Lam, "Exact solution of the problem of quasi-static electric field penetration into a hemispherical indentation in an infinite conducting plane," Interaction Notes, Note 175, April 1974.
- [2] L. Marin, "Quasi-static field penetration into a two-dimensional rectangular well in a ground plane," Interaction Notes, Note 171, March 1974.
- [3] C. Hastings, Jr., Approximations for Digital Computers, Princeton University Press, Princeton, 1955, p. 170.